Brief Review of Linear System Theory

Comment on Project:

You may observe in your system that if you run the fault+line outage simulation to 30 seconds you find a response like this.

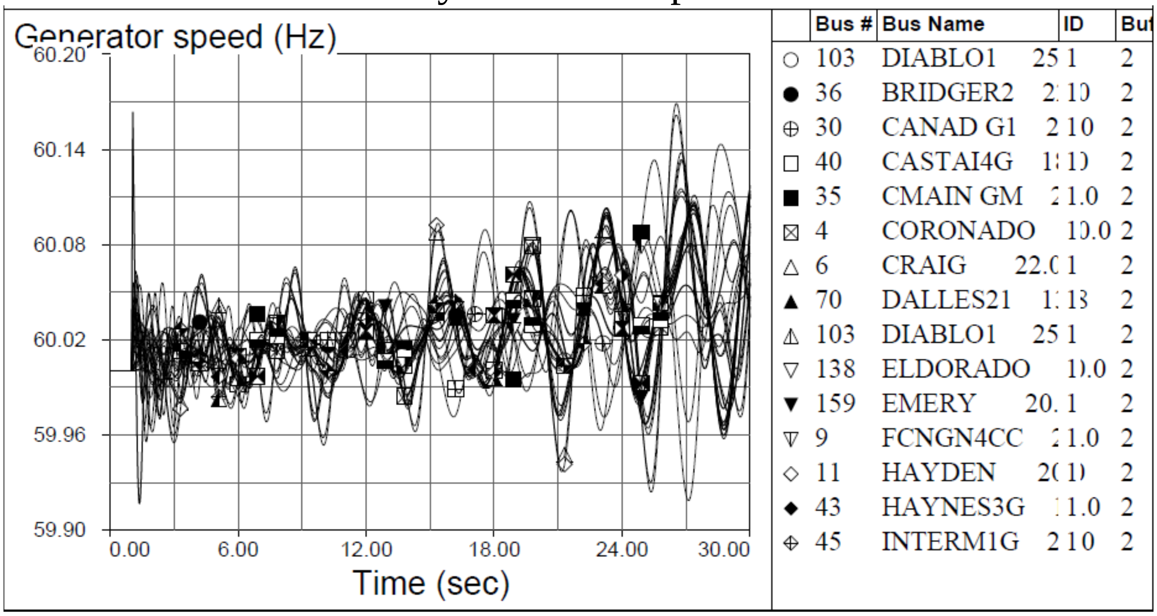

This is due to a right-half-plane pole. It is very hard to find the problem using a time domain simulation tool, but we can do it using an eigenanalysis tool. This is what we will learn about now.

The following information is typically covered in a course on linear system theory. At ISU, EE 577 is one such course and is highly recommended for power system engineering students.

This material is related to VMAF, p. 281-284.

We have developed a model that appears as

$$\underline{\Delta \dot{x}} = \underline{A}\underline{\Delta x}$$

We may write this more compactly as

$$\underline{\dot{x}} = \underline{A}\underline{x}$$

where the "Δ" is implied.

Taking the LaPlace transform, with initial conditions $\underline{x}(0)$, we have:

$$s\underline{X}(s) - \underline{x}(0) = \underline{A}\underline{X}(s)$$

$$\Rightarrow \quad s\underline{X}(s) - \underline{A}\underline{X}(s) = \underline{x}(0)$$

Factoring out the vector $\underline{X}$(s) results in:

$$\left[s\underline{I}-\underline{A}\right]\underline{X}(s)=\underline{x}(0)$$

where $\underline{I}$ is the identity matrix of same dimension as $\underline{A}$.

Pre-multiplying both sides by $[s\underline{I}\text{-}\underline{A}]^{-1}$, we get:

$$\underline{X}(s)=\left[s\underline{I}-\underline{A}\right]^{-1}\underline{x}(0) \qquad \text{(L-1)}$$

and taking the inverse-LaPlace transform leads to

$$\underline{x}(t)=L^{-1}\left\{\left[s\underline{I}-\underline{A}\right]^{-1}\underline{x}(0)\right\} \qquad \text{(L-2a)}$$

Note that in the above, by expressing $[s\underline{I}\text{-}\underline{A}]^{-1}$, we implicitly assume that it is invertible and therefore non-singular (this requires that our system has non-zero determinant).

Recall that a matrix inverse is the adjoint divided by the determinant, i.e., $\underline{K}^{-1}$=Adj($\underline{K}$)/det($\underline{K}$).

Applying this to eq. (L-1), we have:

$$\underline{X}(s)=\frac{\text{Adj}\left\{\left[s\underline{I}-\underline{A}\right]\right\}}{\det\left\{\left[s\underline{I}-\underline{A}\right]\right\}}\underline{x}(0)$$

The determinant of a matrix is a scalar quantity, and in this case, it is a scalar polynomial in the LaPlace variable "*s*" so that:

$$\det\left\{\left[s\underline{I}-\underline{A}\right]\right\}=a_n s^n+a_{n-1}s^{n-1}+\ldots+a_0$$

Such a polynomial may always be factored in the form:

$$\det\left\{\left[s\underline{I}-\underline{A}\right]\right\}=a_n s^n+a_{n-1}s^{n-1}+\ldots+a_0=(s-\lambda_1)(s-\lambda_2)\ldots(s-\lambda_n)$$

L-2b

where the λ_k, k=1, …, n are the roots of the polynomial. Therefore,

$$\underline{X}(s)=\frac{\text{Adj}\left\{\left[s\underline{I}-\underline{A}\right]\right\}}{\det\left\{\left[s\underline{I}-\underline{A}\right]\right\}}\underline{x}(0)=\frac{\text{Adj}\left\{\left[s\underline{I}-\underline{A}\right]\right\}\underline{x}(0)}{(s-\lambda_1)(s-\lambda_2)\ldots(s-\lambda_n)} \qquad \text{(L-3)}$$

Eq. (L-3) expresses the n-dimensional vector $\underline{X}(s)$ as a function of
1. The $n \times n$ matrix Adj[$s\underline{I}$-$\underline{A}$],
2. The $n \times 1$ vector $\underline{x}(0)$
3. The factored polynomial $(s-\lambda_1)(s-\lambda_1)\ldots(s-\lambda_n)$

Note that the numerator is the product of an $n \times n$ matrix and an $n \times 1$ vector and therefore it is $n \times 1$, which is the dimension of the right-hand-side and thus the vector $\underline{X}(s)$. This is as it should be, since $\underline{X}(s)$ is the vector of states, and there should be n states.

If none of the roots λ_k, k=1, …, n are repeated, it will be possible to use partial fraction expansion to express eq. (L-3) in the following way:

$$\underline{X}(s) = \frac{\underline{\mathrm{R}}_1(s)}{(s-\lambda_1)} + \frac{\underline{\mathrm{R}}_2(s)}{(s-\lambda_2)} + \ldots + \frac{\underline{\mathrm{R}}_\mathrm{n}(s)}{(s-\lambda_n)} \tag{L-4}$$

where each $\underline{\mathrm{R}}_\mathrm{k}(s)$ is an $n \times 1$ vector. The inverse LaPlace transform will then appear as:

$$\underline{x}(t) = \underline{r}_1(t)e^{\lambda_1 t} + r_2(t)e^{\lambda_2 t} + \ldots + \underline{r}_n(t)e^{\lambda_n t}$$

The λ_k, k=1,…,n are, in general, complex, such that $\lambda_k=\sigma_k+j\omega_k$.

The λ_k, k=1,…,n are called the system eigenvalues.

We see that the system eigenvalues λ_k, k=1,…,n dictate the nature of the system in terms of the system modal response, where each λ_k corresponds to a system mode. These modes may be oscillatory or non-oscillatory, damped or undamped.

1. Oscillatory:
   - Any mode with $\omega_k \neq 0$ is oscillatory. If there exists an $\lambda_k=\sigma_k+j\omega_k$ such that $\omega_k \neq 0$, then there will exist a corresponding $\lambda_k=\sigma_k-j\omega_k$. These two eigenvalues correspond to the same system mode.
   - Any mode with ω_k=0 is non-oscillatory.

2. Damping: Any mode $\lambda_k=\sigma_k \pm j\omega_k$,
    a. if $\sigma_k>0$, the mode is negatively damped (unstable)
    b. if $\sigma_k<0$, the mode is positively damped (stable)
    c. if $\sigma_k=0$, the mode is marginally damped.

If repeated roots occur in the factorization of (L-2b), then these roots will have time-domain expressions like $t^{r-1}e^{-\lambda t}$ (r is number of repeated roots), and will therefore have the following effects:

a. if $\sigma_k>0$, the mode is negatively damped (unstable)
b. if $\sigma_k<0$, the mode is positively damped (stable); however, the effects of the "t" coefficient might initially dominate the effects of the exponential and cause very large oscillations that could disrupt the system.
c. with $\sigma_k=0$, the effects of the "t" coefficient will result in growing response (unstable)

In practice, it is very unlikely to see repeated roots for power systems. Therefore, we safely assume there are no repeated roots.

<u>Right eigenvectors</u>:

For each eigenvalue, λ_k, k=1,…,n, there exists an n-element column vector $\underline{p}_k$, called a right eigenvector, such that

$$\underline{A}\,\underline{p}_k = \lambda_k \underline{p}_k$$

Since there are n eigenvalues, there are n right eigenvectors.
We may form a matrix of these n right eigenvectors as follows:

$$\underline{P} = \underline{\left\lfloor \underline{p}_1 \quad \cdots \quad \underline{p}_n \right\rfloor}$$

The above matrix, $\underline{P}$, is called the *modal matrix*.

<u>Left eigenvectors</u>:

For each eigenvalue, λ_k, k=1,…,n, there exists an n-element column vector $\underline{q}_k$, called a left eigenvector, such that

$$\underline{q}_k^T \underline{A} = \lambda_k \underline{q}_k^T$$

Since there are n eigenvalues, there are n left eigenvectors.
We may form a matrix of these n left eigenvectors as follows:

$$\underline{Q}^T = \begin{bmatrix} \underline{q}_1^T \\ \vdots \\ \underline{q}_n^T \end{bmatrix}$$

<u>Some properties</u>:

For any two eigenvalues, λ_j, λ_k, then

- For $j \neq k$, q_j and p_k are orthogonal, i.e., their dot product is 0:

$$\underline{q}_j^T \underline{p}_k = 0$$

> Here we define orthogonal *vectors*; recall we previously defined an orthogonal *matrix* to be a square matrix whose columns and rows are orthogonal unit vectors, i.e., $\underline{QQ}^T = \underline{U}$

- For $j = k$,

$$\underline{q}_j^T \underline{p}_j = c_j$$

  where c_j is a constant. A simple scaling of either the right or the left eigenvector will provide that

$$\underline{q}_j^T \underline{p}_j = 1$$

Now consider, based on the above properties, we will get:

$$\underline{Q}^T \underline{P} = \begin{bmatrix} \underline{q}_1^T \\ \vdots \\ \underline{q}_n^T \end{bmatrix} \begin{bmatrix} \underline{p}_1 & \cdots & \underline{p}_n \end{bmatrix} = \begin{bmatrix} \underline{q}_1^T \underline{p}_1 & \underline{q}_1^T \underline{p}_2 & \underline{q}_1^T \underline{p}_3 & \cdots & \underline{q}_1^T \underline{p}_n \\ \underline{q}_2^T \underline{p}_1 & \underline{q}_2^T \underline{p}_2 & \underline{q}_2^T \underline{p}_3 & \cdots & \underline{q}_2^T \underline{p}_n \\ \underline{q}_3^T \underline{p}_1 & \underline{q}_3^T \underline{p}_2 & \underline{q}_3^T \underline{p}_3 & \cdots & \underline{q}_3^T \underline{p}_n \\ \vdots & \vdots & \vdots & \cdots & \vdots \\ \underline{q}_n^T \underline{p}_1 & \underline{q}_n^T \underline{p}_2 & \underline{q}_n^T \underline{p}_3 & \cdots & \underline{q}_n^T \underline{p}_n \end{bmatrix} = \begin{bmatrix} \underline{q}_1^T \underline{p}_1 & 0 & 0 & \cdots & 0 \\ 0 & \underline{q}_2^T \underline{p}_2 & 0 & \cdots & 0 \\ 0 & 0 & \underline{q}_3^T \underline{p}_3 & \cdots & 0 \\ \vdots & \vdots & \vdots & \cdots & \vdots \\ 0 & 0 & 0 & \cdots & \underline{q}_n^T \underline{p}_n \end{bmatrix}$$

We can go a step further if the scaling is performed:

$$\underline{Q}^T \underline{P} = \underline{I}$$

Post-multiplying both sides by $\underline{P}^{-1}$ results in

$$\underline{Q}^T = \underline{P}^{-1}$$

Note that neither Q or P are orthogonal matrices, but $Q^T P$ is. Also:

- $\underline{PP}^{-1} = \underline{I}$
- $[\underline{Q}^T]^{-1} \underline{Q}^T = \underline{I}$

We can illustrate calculation of the right and left eigenvectors using the sample system given in the book (fig. 2.19, and example 3.2), having state-space model of

$$\begin{bmatrix} \Delta\dot{\delta}_{13} \\ \Delta\dot{\delta}_{23} \\ \Delta\dot{\omega}_{13} \\ \Delta\dot{\omega}_{23} \end{bmatrix} = \underbrace{\begin{bmatrix} 0 & 0 & 1 & 0 \\ 0 & 0 & 0 & 1 \\ -104.096 & -59.524 & 0 & 0 \\ -33.841 & -153.460 & 0 & 0 \end{bmatrix}}_{\underline{A}} \begin{bmatrix} \Delta\delta_{13} \\ \Delta\delta_{23} \\ \Delta\omega_{13} \\ \Delta\omega_{23} \end{bmatrix}$$

You can compute eigenvalues of this matrix in Matlab as follows:

```
>> A=[0 0 1 0; 0 0 0 1; -104.096 -59.524 0 0; -33.841 -153.460 0 0]

A =

         0         0    1.0000         0
         0         0         0    1.0000
 -104.0960  -59.5240         0         0
  -33.8410 -153.4600         0         0

>> eig(A)

ans =

  -0.0000 +13.4164i
  -0.0000 -13.4164i
   0.0000 + 8.8067i
   0.0000 - 8.8067i
```

Observe the eigenvalues in Table 3.2

Table 3.2. Frequencies of Oscillation of a Nine-Bus System

Quantity	Eigenvalue 1	Eigenvalue 2
λ	$\pm j8.807$	$\pm j13.416$
ω rad/s	8.807	13.416
f Hz	1.402	2.135
T s	0.713	0.468

Also observe the relative rotor angle plots of fig. 3.3-b, for the case when a small load was added to bus #8. Here we see that one mode

can be clearly observed having a period of about 0.7 sec (f=1.4Hz, $\omega=2\pi f$=8.8 rad/sec).
The other mode (2.1Hz) is not readily observable, although its presence is likely responsible for the distortion seen in the δ_{31} plot.

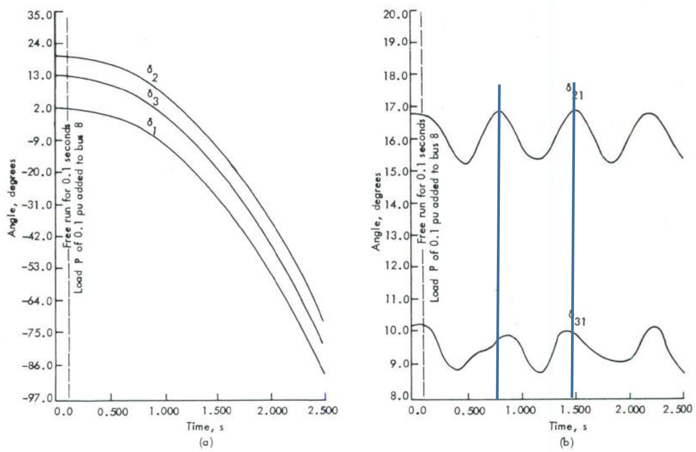

Fig. 3.3 Unregulated response of the nine-bus system to a sudden load application at bus 8: (a) absolute angles, (b) angles relative to δ_1.

From matlab, we use
[P,D]=eig(A) where A is the matrix $\underline{A}$ given above.

Then the matrix of eigenvalues D is given by

+13.4164i	0	0	0
0	-13.4164i	0	0
0	0	+8.8067i	0
0	0	0	- 8.8067i

And the matrix of right eigenvectors P is given by

-0.0459 - 0.0000i	-0.0459 + 0.0000i	-0.1030 - 0.0000i	-0.1030 + 0.0000i
-0.0585 - 0.0000i	-0.0585 + 0.0000i	0.0459 + 0.0000i	0.0459 - 0.0000i
0.0000 - 0.6154i	0.0000 + 0.6154i	0.0000 - 0.9075i	0.0000 + 0.9075i
0.0000 - 0.7847i	0.0000 + 0.7847i	-0.0000 + 0.4046i	-0.0000 - 0.4046i

And the matrix of left eigenvectors Q^T is given by P^{-1}, which is:

-2.8240 + 0.0000i	-6.3340 + 0.0000i	0.0000 + 0.2105i	0.0000 + 0.4721i
-2.8240 - 0.0000i	-6.3340 - 0.0000i	0.0000 - 0.2105i	0.0000 - 0.4721i
-3.5951 + 0.0000i	2.8194 - 0.0000i	0.0000 + 0.4082i	-0.0000 - 0.3201i
-3.5951 - 0.0000i	2.8194 + 0.0000i	0.0000 - 0.4082i	-0.0000 + 0.3201i

Note that here, the eigenvectors are along the rows. Taking transpose, we get Q, which is

-2.8240 + 0.0000i	-2.8240 - 0.0000i	-3.5951 + 0.0000i	-3.5951 - 0.0000i
-6.3340 + 0.0000i	-6.3340 - 0.0000i	2.8194 - 0.0000i	2.8194 + 0.0000i
0.0000 + 0.2105i	0.0000 - 0.2105i	0.0000 + 0.4082i	0.0000 - 0.4082i
0.0000 + 0.4721i	0.0000 - 0.4721i	-0.0000 - 0.3201i	-0.0000 + 0.3201i

In the above, the left eigenvectors are the columns.

Note also that the columns of right (or left) eigenvectors corresponding to complex conjugate eigenvalues are complex conjugate eigenvectors.

The numerators of eq. (L-4)

Let's return to eq. (L-4), which is restated here for convenience:

$$\underline{X}(s) = \frac{\underline{\mathrm{R}}_1(s)}{(s+\lambda_1)} + \frac{\underline{\mathrm{R}}_2(s)}{(s+\lambda_2)} + \ldots + \frac{\underline{\mathrm{R}}_\mathrm{n}(s)}{(s+\lambda_n)}$$

What are these $\underline{\mathrm{R}}_\mathrm{k}$, k=1,…,n?

To answer this, let's return to eq. (L-1), which is:

$$\underline{X}(s) = [s\underline{I} - \underline{A}]^{-1}\underline{x}(0)$$

Let's pre-multiply the right-hand side by $\underline{P}\underline{P}^{-1}$ and post-multiply the right-hand-side by $[\underline{Q}^T]^{-1}\,\underline{Q}^T$. This is acceptable, since both of these products yield the identity. This results in:

$$\underline{X}(s) = \underline{P}\,\underline{P}^{-1}[s\underline{I} - \underline{A}]^{-1}\left[\underline{Q}^T\right]^{-1}\underline{Q}^T\,\underline{x}(0)$$

Bracket the inner products:

$$\underline{X}(s) = \underline{P}\left\{\underline{P}^{-1}[s\underline{I} - \underline{A}]^{-1}\left[\underline{Q}^T\right]^{-1}\right\}\underline{Q}^T\,\underline{x}(0)$$

We can show that what is inside the (highlighted) curly brackets is:

$$[s\underline{I} - \underline{\Lambda}]^{-1} = \underline{P}^{-1}[s\underline{I} - \underline{A}]^{-1}\left[\underline{Q}^T\right]^{-1}$$

where

$$\underline{\Lambda} = \mathrm{diag}(\lambda_k)$$

The proof is below:

[1]Since A is square and assumed to have distinct eigenvalues, it has full rank. Given that P is the matrix of N independent right eigenvectors, A may be diagnalized by

$$P^{-1}AP = \Lambda = diag(\lambda_i)$$

Since the right and left eigenvector matricies P and Q^T are orthogonal, $P = [Q^T]^{-1}$, and

$$P^{-1}A[Q^T]^{-1} = \Lambda = diag(\lambda_i)$$

If P and Q^T are the right and left eigenvector matricies for A, then they are also the right and left eigenvector matricies for $[sI - A]$. Therefore

$$P^{-1}[sI - A][Q^T]^{-1} = [sI - \Lambda]$$

Recalling $[BCD]^{-1} = D^{-1}C^{-1}B^{-1}$, both sides of the previous equation may be inverted to yield

$$Q^T[sI - A]^{-1}[P] = [sI - \Lambda]^{-1}$$

Again using the orthogonality condition $P = [Q^T]^{-1}$,

$$P^{-1}[sI - A]^{-1}[Q^T]^{-1} = [sI - \Lambda]^{-1}$$

Then, we have that:

$$\overbrace{\underline{X}(s)}^{n\times 1} = \overbrace{\underline{P}}^{n\times n} \overbrace{\left\{\left[s\underline{I} - \underline{\Lambda}\right]^{-1}\right\}}^{n\times n} \overbrace{\underline{Q}^T}^{n\times n} \overbrace{\underline{x}(0)}^{n\times 1} \qquad (*\#)$$

Two comments are relevant at this point:

1. The matrix being inverted is a diagonal matrix. Therefore, the matrix inverse is obtained by inverting each diagonal element.
2. Recall the orthogonality property $\underline{p}_i\underline{q}_j=0$ for $i\neq j$.

Using these comments, we can perform the matrix multiplication on (*#) to obtain:

$$\underline{X}(s) = \underline{P}\left[s\underline{I} - \underline{\Lambda}\right]^{-1}\left[\underline{Q}^T\right]\underline{x}(0) = \left[\underline{p}_1 \quad \underline{p}_2 \quad \underline{p}_3 \quad \cdots \quad \underline{p}_n\right] \begin{bmatrix} \frac{1}{s-\lambda_1} & 0 & 0 & 0 & 0 \\ 0 & \frac{1}{s-\lambda_2} & 0 & 0 & 0 \\ 0 & 0 & \frac{1}{s-\lambda_3} & 0 & 0 \\ \vdots & \vdots & \vdots & \cdots & \vdots \\ 0 & 0 & 0 & 0 & \frac{1}{s-\lambda_n} \end{bmatrix} \begin{bmatrix} \underline{q}_1^T \\ \underline{q}_2^T \\ \underline{q}_3^T \\ \vdots \\ \underline{q}_n^T \end{bmatrix} \underline{x}(0)$$

$$= \left[\frac{\underline{p}_1}{s-\lambda_1} \quad \frac{\underline{p}_2}{s-\lambda_2} \quad \frac{\underline{p}_3}{s-\lambda_3}\underline{p}_3 \quad \cdots \quad \frac{\underline{p}_n}{s-\lambda_n}\right] \begin{bmatrix} \underline{q}_1^T\underline{x}(0) \\ \underline{q}_2^T\underline{x}(0) \\ \underline{q}_3^T\underline{x}(0) \\ \vdots \\ \underline{q}_n^T\underline{x}(0) \end{bmatrix} = \sum_{k=1}^{n}\frac{\underline{p}_k\underline{q}_k^T\underline{x}(0)}{s-\lambda_k}$$

$$\underline{X}(s) = \sum_{k=1}^{n} \frac{\underline{p}_k \overbrace{(\underline{q}_k^T \underline{x}(0))}^{1\times 1}}{s-\lambda_k} = \sum_{k=1}^{n} \frac{(\underline{q}_k^T \underline{x}(0))\underline{p}_k}{s-\lambda_k}$$

Taking the inverse LaPlace transform, we obtain:

$$\underline{x}(t) = \sum_{k=1}^{n} \left[\underline{q}_k^T \underline{x}(0) e^{\lambda_k t}\right] \underline{p}_k \qquad \text{(L-5)}$$

This is a very important relationship. It shows how we can use the right eigenvalue to determine the *shape* of the k^{th} mode.

To understand mode shape, focus on *a single term* in the summation, the k^{th} term; this term is entirely responsible for mode k dynamics in the time-domain response of each state. Call it $\underline{x}_k(t)$, given by

$$\underline{x}_k(t) = \left[\underline{q}_k^T \underline{x}(0) e^{\lambda_k t}\right] \underline{p}_k \qquad \text{(L-6a)}$$

Inspecting eq. (L-6a), we see that the right eigenvector $\underline{p}_k$ determines the relative distribution of the mode through the state variables $x_k(t)$. To see this, note that

- $\underline{p}_k$ and $\underline{x}_k(t)$ are both $n\times 1$ vectors, with element i corresponding to the i^{th} state variable;
- $\underline{q}_k^T \underline{x}(0) e^{\lambda_k t}$ is scalar and multiplies every element of $\underline{p}_k$; so it does not distinguish any state any differently than another state;
- $\underline{p}_k$ is therefore the only thing that distinguishes one state from another in terms of the mode k dynamics.

These observations become more apparent if we expand (L6-a) to:

$$\Rightarrow \begin{bmatrix} x_{k1}(t) \\ x_{k2}(t) \\ x_{k3}(t) \\ x_{k4}(t) \end{bmatrix} = \underline{x}_k(t) = \left[\underline{q}_k^T \underline{x}(0) e^{\lambda_k t}\right] \underline{p}_k = \left[\underline{q}_k^T \underline{x}(0) e^{\lambda_k t}\right] \begin{bmatrix} p_{k1} \\ p_{k2} \\ p_{k3} \\ p_{k4} \end{bmatrix} \text{(L-6b)}$$

If the states are limited to only the generator inertial states $\Delta\delta$ and $\Delta\omega$, then each element of $\underline{p}_k$ gives the relative distribution of the mode in a particular generator's angle or speed.

Caution: Although the right eigenvector shows us how gens swing against each other, it does NOT tell us how much a state influences a mode, i.e., $\underline{p}_k$ does not tell which machines are most effective to control the mode.

The right eigenvector does tell you the ***relative phase*** of each state in that mode. If you "plot" each element (a complex number and thus interpretable as a vector) corresponding to each $\Delta\omega$ state (one for each generator) in the right eigenvector $\underline{p}_k$, you can see which generators are swinging against one another. This is called **mode shape**. Relative phases can be observed in time domain simulations.

Some interesting ways of illustrating the relative phase of each $\Delta\omega_k$ as determined by the $\underline{p}_k$'s are shown in:

- Klein, Rogers, and Kundur, "A fundamental study of interarea oscillations in power systems," IEEE Trans Power Sys, V. 6, No. 3, Aug 1991 (its on website). See the two pages below. Fig. 2 shows the mode shape where gens 1,2 swing against gens 11,12, and in the time domain simulation, Fig. 3.

3.0 METHODS OF ANALYSIS

Both small signal stability analysis and transient stability analysis were used, in a complementary way, in our study of inter-area oscillations. Small signal stability analysis, using modal techniques [7], is most appropriate for determining the nature of inter-area modes in power systems. In this case, the system studied was small enough to allow the analysis of all system modes, using MASS computer program [8]. The system eigenvalues, eigenvectors, and participation factors [7] were computed for a number of different system conditions and configurations.

In some instances, in particular in our investigation of the effects of loads, we found it useful to augment the small signal stability analysis with transient stability runs. The graphic nature of the output of the transient stability program aids in picturing the pattern of voltage oscillations, and their relationship with the eigenvectors calculated using modal analysis.

4.0 EFFECTS OF TIE LINE IMPEDANCE AND FLOW

In these tests, all four generating units were represented identically by detailed generator and fast static exciter models. All loads were represented as constant impedances. The tie line impedance was varied by changing the number of tie circuits in service. Power transfers between the two areas were created, either by an uneven distribution of generation between the areas, or by an uneven split of the total system load.

4.1 Effect on Frequency and Damping

The frequency and damping ratio of the inter-area mode for various combinations of tie line power flow and number of tie circuits in service are given in Table 1. As is to be expected: the frequency and damping ratio, of the inter-area mode, drop as the tie line impedance or power flow is increased.

TABLE 1
Effects of Tie Line Impedance and Flow on Frequency and Damping of the Inter-Area Mode

POWER FLOW AREA 1 to 2 (MW)	TIES I/S	GENERATION/LOAD AREA 1	AREA 2	FREQ (Hz)	DAMPING RATIO
0	3	1400/1367	1400/1367	0.748	0.018
"	2	"	"	0.661	0.011
"	1	"	"	0.513	0.002
400	3	1400/967	1450/1767	0.732	0.015
600	3	1400/767	1457/1967	0.683	0.008
400	1	1400/967	1450/1767	0.359	-0.002
380	1	1800/1367	1045/1367	0.363	-0.021

4.2 Effect on Mode Shape

The normalized eigenvector components, corresponding to rotor speeds, of the inter-area mode, for various tie line impedances and power flows, are shown in Figure 2. The results lead to the following conclusions.

1. In a symmetric system with no power transfer between the two areas, as in tests 1 and 2, the generating units in one area oscillate exactly in anti-phase to the ones in the second area (generator 1 versus 11, and 2 versus 12). The units which oscillate in anti-phase, have the same amplitude. The outer units oscillate more than the inner ones.

2. In an asymmetric system, as in test 3, where the generation in each area supplies the area load and hence, there is no flow on the tie line, the phase difference between the generating units in the two areas is slightly less than 180°.

3. In an asymmetric system with power flow on the tie line, as in tests 4 and 5, the phase difference between the generating units in the two areas is noticeably less than 180°, about 150° in this case. The generating units in the receiving area oscillate with a higher amplitude than the ones in the sending area.

Results of time domain simulations for the systems in test 2 and 4 are shown in Figures 3 and 4 respectively. These results correlate well with those of the eigenvalue/vector analysis.

5.0 EFFECT OF EXCITATION SYSTEMS

5.1 Effect on Frequency and Damping

To test the effect of the excitation systems on the frequency and damping of the inter-area mode we carried out two sets of tests: one set with identical exciters on all four units and the other set with one fast exciter and three slow or manually controlled exciters.

5.1.1 Tests with Identical Exciters

In this set of tests we explored the effect of the following four types of exciters on the inter-area mode:

- Manually controlled exciters
- Slow dc exciters
- Fast static exciters with and without transient gain reduction (TGR).

Only the automatic voltage regulator effects were investigated. Other controls, such as power system stabilizers, were not considered.

We considered two operating conditions: a stressed system with only one tie circuit I/S and 400 MW power transfer from Area 1 to 2, and an unstressed system with no power transfer between the areas. Constant impedance loads were assumed in these tests.

The results, summarized in Table 2, show that the inter-area mode is best damped with manually controlled exciters, and worst damped with fast exciters with TGR. The frequency is highest for fast exciters without TGR and lowest for slow exciters.

TEST	1	2	3	4	5
TEST I/S	3	1	1	1	1
AREA 1 GEN./LOAD	1400 / 1367	1400 / 1367	1120 / 1100	1400 / 967	1800 / 1367
AREA 2 GEN./LOAD	1400 / 1367	1400 / 1367	1700 / 1650	1450 / 1767	1045/ 1367
FLOW AREA 1 TO 2 (MW)	0	0	0	400	380

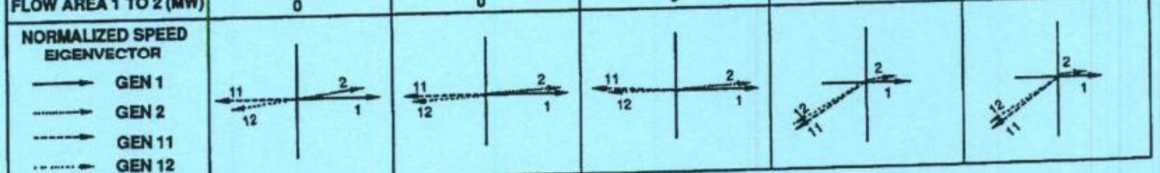

FIGURE 2
Effect of Tie Line Impedance and Flow on Mode Shape

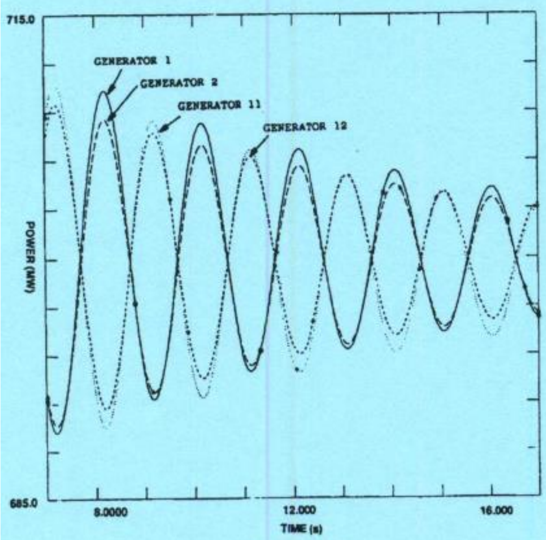

FIGURE 3
Generators' Active Power

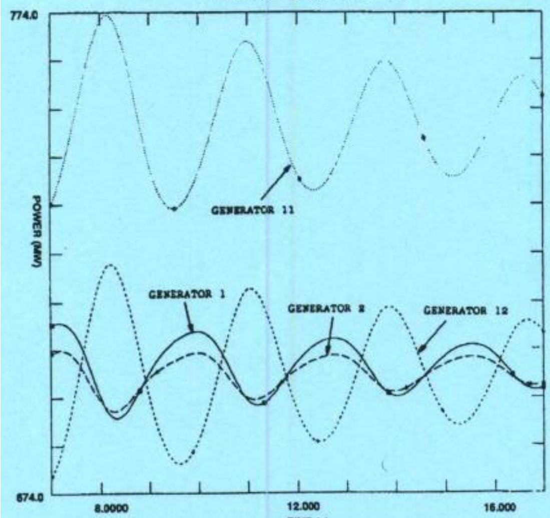

FIGURE 4
Generators' Active Power

5.1.2 Tests with One Fast Exciter

One slow, or manually controlled exciter, was replaced in turn with a fast exciter, with the objective of studying the impact that the relative locations of the generating unit have. Except for the exciter, the generating units are identical; therefore, the differences in the results of the tests are due only to the location of the generating unit having the fast exciter.

The results, summarized in Table 3, lead to the following conclusions:

1. The effect of one fast exciter on the damping of the inter-area mode depends on its location and on the other types of exciters in the system.

   In the case of one fast exciter and three manually controlled exciters, a fast exciter in the receiving area significantly improves the damping of the mode, while a fast exciter in the sending area reduces the damping. In the case of one fast exciter and three slow exciter the opposite is true.

2. The effect of a fast exciter on the frequency of the inter-area mode depends on the location of the exciter. A fast exciter in the sending area increases the frequency, while one in the receiving area reduces it.

In an attempt to understand these results, we examined the open loop (no AVR) transfer function between field voltage and terminal voltage ($E_t(s)/E_{fd}(s)$) for GEN 2 and GEN 12 under various power transfers between the areas and found that this transfer function has a zero around 0.3 Hz. Obviously, when there is no flow on the tie line, this transfer function for GEN 2 is identical to that for GEN 12. As the flow on the tie line is increased, these two transfer functions begin to differ mainly in terms of this zero. When the loop is closed through the exciter, the inter-area pole migrates towards this zero and so causing the difference in the effect of the fast exciter on GEN 2 and GEN 12.

For example, in the case of manually controlled exciters, with no flow on the tie line, the zero has a negative real part. As the inter-area power transfer is increased, the zero associated with the transfer function of the sending area generator, GEN 2, moves to the right and crosses into the right half of the s-plane. The zero associated with the transfer function of the generator in the receiving area, GEN 12, moves to the left.

TABLE 2
Effect of Excitation Systems on Frequency and Damping of the Inter-Area Mode

POWER FLOW AREA 1 to 2 (MW)	EXCITER MODEL	FREQ (Hz)	DAMPING RATIO
0	MANUALLY CONTROLLED	0.481	0.023
"	FAST WITHOUT TGR	0.513	0.002
"	FAST WITH TGR	0.485	-0.016
"	SLOW	0.470	0.004
400	MANUALLY CONTROLLED	0.340	0.033
"	FAST WITHOUT TGR	0.358	-0.002
"	FAST WITH TGR	0.341	-0.017
"	SLOW	0.330	0.009

TABLE 3
Effect of One Fast Exciter on the Inter-Area Mode

	EXCITERS ON THE REMAINING UNITS			
	SLOW		MANUALLY CONTROLLED	
GENERATOR WITH FAST EXCITER	FREQ (Hz)	DAMPING RATIO	FREQ (Hz)	DAMPING RATIO
None	0.330	0.009	0.340	0.033
1	0.419	0.019	0.388	-0.048
2	0.467	-0.010	0.440	-0.062
11	0.286	-0.163	0.289	0.140
12	0.241	-0.283	0.208	0.357

5.2 Effect on Mode Shape

The effect of different generator and excitation system models on the mode shape were explored under two operating conditions: an unstressed system with no power flow on the tie, and a stressed system with 400 MW flow from Area 1 to Area 2 on a single tie circuit.

The following alternative generator-excitation system models were considered:

- Classical machine model (Fixed voltage behind transient reactance)
- Detailed machine model with a manually controlled exciter
- Detailed machine model with a fast exciter (no TGR)
- Detailed machine with a slow exciter

The results of these tests are depicted in Figure 5. It can be seen that in a symmetric system, with no power flow on the tie line, the generating units in one area oscillate in anti-phase to those in the

- Also, from Wang, Howell, Kundur, Chung, and Xu, "A tool for small-signal security assessment of power systems," on website. See mode shape, Fig. 5.

No.	Frequency (Hz)	Damping Ratio (%)
1	0.306	8.53
2	0.366	3.92
3	0.380	2.31
4	0.416	3.51
5	0.446	3.04
6	0.468	3.60
7	0.549	2.51
8	0.563	3.82
9	0.600	3.95

Table 3 – Interarea modes of Test System 2

Figure 5 shows the mode shape of the first mode (at 0.306 Hz). Each symbol in the figure represents the normalized right eigenvector entry for a generator. From this mode shape, it is seen that the generators in the eastern portion of the system have a large phase angle (close to 180°) against the generators in the western portion of the system. Therefore, this mode represents an east-west (interarea) oscillation in the system.

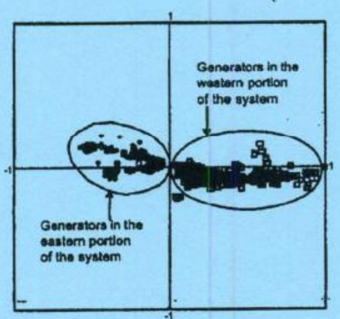

Figure 5 – Mode shape of the 0.306 Hz mode

Computation of a specified local mode

The objective of this example is to find the local mode at the Rush Island generating units in the Ameren UE area. This mode is the focus of several investigations [10] after the oscillation incident in 1992 involving the Rush Island units.

This mode occurred as a result of a contingency that effectively disconnected two of three circuits connecting the Rush Island units to the rest of the system. Under this condition, a local mode around 1 Hz at Rush Island may become poorly damped to cause sustained oscillations. To find this mode, the option in SSAT to compute modes related to a generator is used, after applying the contingency to the base case. This mode turns out to be at 1.28 Hz with a damping ratio of 4.19%. Figure 6 shows a time-domain simulation verification performed using the full nonlinear simulation in which one of the Rush Island unit speed is plotted. The simulation clearly shows an oscillation at about 1.3 Hz.

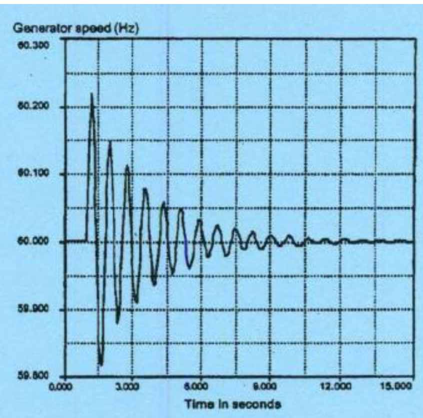

Figure 6 – Simulation verification of the Rush Island mode

The significance of this example is to show the capability of SSAT to selectively compute local modes in a large model. Using the usual eigenvalue analysis approach, this kind of computation would likely need preliminary model reduction work, or an extensive mode scan in the crowded local mode frequency range. Being able to directly locate the required mode with the base study model helps significantly improve the efficiency of the studies.

VI. CONCLUSIONS

This paper presents a tool (SSAT) for small-signal security assessment of power systems. It is developed as a result of the calls from the power industry for a program to meet the increasing need of system studies. The focus of this development has been to provide superior modelling support and capabilities for the security assessment, while taking advantages of the recent advancement in the basic computational algorithm development (such as eigenvalue solvers). The theoretical foundations of SSAT are described and its computational capabilities illustrated with numerical examples.

VII. ACKNOWLEDGEMENT

This work is co-funded by Allegheny Power, AmerenUE, BC Hydro, Entergy Services Inc., Florida Power & Light Co., Manitoba Hydro, and Minnesota Power. Technical advises and reviews from representatives of these utilities are greatly appreciated. The authors are also grateful to their colleagues at Powertech Labs Inc. for valuable help to the SSAT development.

REFERENCES

[1] P. Kundur, *Power System Stability and Control*, McGraw-Hill, 1994

- And from Y. Mansour, “Application of eigenanalysis to the Western North American Power system,” on website. Tables 4, 5, and 6, each table for a certain condition, give eigenvector elements for speed deviation at each of a number of generators. Figures 1, 2, and 3 show, for three conditions, geographical plots of the mode shapes for 4 different modes.

Table 1

LOW FREQUENCY MODES
REDUCED ORDER SYSTEM MODEL

EIGEN VALUE	FREQUENCY (Hz)
− 0.094 + J 1.73	0.275
− 0.131 + J 2.77	0.44
− 0.124 + J 2.89	0.46
− 0.84 + J 3.54	0.564
− 0.102 + J 3.7	0.588
− 0.089 + J 4.18	0.665
− 0.095 + J 4.42	0.704
− 0.134 + J 4.78	0.76
− 0.123 + J 5.17	0.823
− 0.177 + J 5.31	0.845
− 0.227 + J 5.62	0.895
− 0.163 + J 5.7	0.907
− 0.147 + J 5.94	0.946
− 0.092 + J 6.00	0.955
− 0.173 + J 6.27	0.998

Table 2

1988 HEAVY WINTER CASE
NORMAL SYSTEM
EIGEN VALUES

CASE #1	CASE #2
-0.0934 + J 3.78 : 0.6 Hz	-0.19 + J 3.83 : 0.61 Hz
-0.1098 + J 4.58 : 0.729 Hz	-0.2078 + J 4.788 : 0.762 Hz
-0.1168 + J 4.66 : 0.741 Hz	-0.704 + J 4.8 : 0.765 Hz
-0.1278 + J 4.90 : 0.781 Hz	-0.366 + J 4.89 : 0.778 Hz
CASE #3	**CASE #4**
-0.26 + J 3.7 : 0.59 Hz	-0.197 + J 3.796 : 0.604 Hz
-0.361 + J 4.71 : 0.75 Hz	-0.1467 + J 4.747 : 0.756 Hz
-0.282 + J 4.91 : 0.78 Hz	-0.39 + J 4.787 : 0.762 Hz
-0.636 + J 4.93 : 0.784 Hz	-0.536 + J 5.036 : 0.802 Hz

CASE #1 : GENERATORS ONLY, NO CONTROL.
CONSTANT I MW AND CONSTANT Z MVAR LOAD.

CASE #2 : GENERATORS, EXCITERS, PSS's, AND GOV.
CONSTANT I MW AND CONSTANT Z MVAR LOAD.

CASE #3 : GENERATORS, EXCITERS, PSS's, AND GOV.
CONSTANT Z MW AND CONSTANT Z MVAR LOAD.

CASE #4 : SAME AS CASE #2 PLUS D.C. LINKS MODEL.

Table 3

1988 HEAVY WINTER CASE
ABNORMAL SYSTEM
EIGEN VALUES

CASE #5	CASE #6
-0.2100 + J 3.78 : 0.6 Hz	-0.20 + J 3.81 : 0.61 Hz
-0.0566 + J 4.43 : 0.721 Hz	-0.1470 + J 4.620 : 0.735 Hz
-0.3840 + J 4.77 : 0.760 Hz	-0.400 + J 4.88 : 0.777 Hz
-0.5396 + J 5.07 : 0.807 Hz	-0.680 + J 4.84 : 0.770 Hz
CASE #7	**CASE #8**
-0.20 + J 3.74 : 0.60 Hz	-0.233 + J 3.74 : 0.6 Hz
-0.075 + J 4.62 : 0.73 Hz	+0.030 + J 4.30 : 0.68 Hz
-0.391 + J 4.78 : 0.76 Hz	-0.381 + J 4.74 : 0.755 Hz
-0.492 + J 4.97 : 0.791 Hz	-0.81 + J 5.06 : 0.8 Hz

CASE #4*
-0.197 + J 3.796 : 0.604 Hz
-0.1467 + J 4.747 : 0.756 Hz
-0.39 + J 4.787 : 0.762 Hz
-0.536 + J 5.036 : 0.802 Hz

CASE #5 : PALO VERDE - DEVERS 500 kV LINE OUT OF SERVICE.
MACHINES, EXCITERS, PSS's, GOV, AND D.C.
CONSTANT I MW AND CONSTANT Z MVAR LOAD.

CASE #6 : SAME AS CASE #5 BUT WITHOUT D.C. MODEL.

CASE #7 : BLOCK BIPOLE D.C., REST OF THE SYSTEM NORMAL.
CONSTANT I MW AND CONSTANT Z MVAR LOAD.

CASE #8 : BLOCK BIPOLE D.C., PALO VERDE - DEVERS O.O.S.
CONSTANT I MW AND CONSTANT Z MVAR LOAD.

* REPEATED HERE FOR COMPARISON.

Table 4

1988 HEAVY WINTER CASE
PALO VERDE - DEVERS LINE OUT OF SERVICE
0.72 Hz MODE (−0.057 + J 4.43)

EIGEN VECTOR				PARTICIPATION VECTOR		
GEN	AREA	MAG	PH	GEN	AREA	MAG
GEYSER34	PG&E	1.0	-176	HELMS G	PG&E	1.0
HELMS G	PG&E	0.9	169	BIGCREEK	S.CAL	0.6
GEYSER78	PG&E	0.9	-176	KEMANO	B.C.	0.5
BIGCREEK	S.CAL	0.8	-165	GEYSER D	PG&E	0.4
MELONES	PG&E	0.7	-156	FCNGN4CC	ARIZ	0.3
GEYSER B	PG&E	0.7	-175	RNCHSECO	PG&E	0.3
GEYSER D	PG&E	0.7	-176	GEYSER C	PG&E	0.3
GEYSER A	PG&E	0.6	-175	MOSS 7	PG&E	0.3
GEYSER C	PG&E	0.6	-176	GEYSER B	PG&E	0.2
FOLSOM1	PG&E	0.6	-178	MELONES	PG&E	0.2
FOLSOM23	PG&E	0.6	-178	GEYSER34	PG&E	0.2
KERCKHOF	PG&E	0.6	-179	DIABLO1	PG&E	0.2
	"			GEYSER78	PG&E	0.2
	"			DIABLO2	PG&E	0.2
--------				PTS7SWNG	PG&E	0.2
				COMANCHE	COLRD	0.2
INTERM2G	UTAH	0.3	19.5			
EHUNTR 1	UTAH	0.2	5.0			
INTERM1G	UTAH	0.3	18.5			
EHUNTR 2	UTAH	0.2	4.8			
NEWMANG6	N.MEX	0.3	-25.4			
MOHAV2CC	S.CAL	0.3	-22.3			
MOHAV1CC	S.CAL	0.3	-22.3			
APACHCT3	ARIZ	0.3	-21.5			
FCNGN4CC	ARIZ	0.3	-26.8			
HOVRA3A4	WAPA	0.4	-17.4			
NEWMAN45	N.MEX	0.5	-32.3			
BLNDL G1	UTAH	0.5	4.5			

Table 5

1988 HEAVY WINTER CASE
BLOCK BIPOLE D.C. LINK
0.73 Hz MODE (−0.075 + J 4.62)

EIGEN VECTOR				PARTICIPATION VECTOR		
GEN	AREA	MAG	PH	GEN	AREA	MAG
GEYSER34	PG&E	1.0	6.6	HELMS G	PG&E	1.0
GEYSER78	PG&E	0.9	6.9	GEYSER D	PG&E	0.6
HELMS G	PG&E	0.8	-9.2	GEYSER C	PG&E	0.5
GEYSER B	PG&E	0.6	7.3	RNCHSECO	PG&E	0.4
GEYSER D	PG&E	0.6	7.6	FCNGN4CC	ARIZ	0.3
GEYSER A	PG&E	0.6	6.8	GEYSER34	PG&E	0.3
GEYSER C	PG&E	0.6	7.5	MOSS 7	PG&E	0.3
MELONES	PG&E	0.6	-22	GEYSER B	PG&E	0.3
FOLSOM1	PG&E	0.6	5.3	KEMANO	B.C.	0.2
FOLSOM23	PG&E	0.6	5.0	GEYSER78	PG&E	0.2
POTRERO3	PG&E	0.5	5.1	MELONES	PG&E	0.2
ROCKCREQ	PG&E	0.5	5.9	NEWMAN46	N.MEX	0.2
	"			PTS7SWNG	PG&E	0.2
--------	"			HYATTGEN	PG&E	0.2
				SHASTA	PG&E	0.2
PEGS1	N.MEX	0.3	162.4			
APACHST3	ARIZ	0.3	167.9			
HOVRA5-7	WAPA	0.3	179.4			
MOHAV2CC	S.CAL	0.3	156.3			
MOHAV1CC	S.CAL	0.3	156.3			
FCNGN4CC	ARIZ	0.3	153.6			
ELBUTTEG	N.MEX	0.3	166.5			
HOVRA3A4	WAPA	0.3	176.5			
NEWMANG3	N.MEX	0.3	163.6			
FCNGN4CC	ARIZ	0.5	131.6			
NEWMANG2	N.MEX	0.3	162.4			
NEWMANG6	N.MEX	0.4	163.5			
APACHCT3	ARIZ	0.4	169.6			
BLNDL G1	UTAH	0.4	158.3			
NEWMAN45	N.MEX	0.6	156.5			

Table 6

1988 HEAVY WINTER CASE
BLOCK BIPOLE D.C. LINK
PALO VERDE − DEVERS O.O.S.
0.68 Hz MODE (+0.030 + J 4.30)

EIGEN VECTOR				PARTICIPATION VECTOR		
GEN	AREA	MAG	PH	GEN	AREA	MAG
GEYSER34	PG&E	1.0	0.6	HELMS G	PG&E	1.0
GEYSER78	PG&E	0.9	1.2	GEYSER D	PG&E	0.5
HELMS G	PG&E	0.8	-11.	BIGCREEK	S.CAL	0.6
BIGCREEK	S.CA	0.8	9.8	KEMANO	B.C.	0.4
MELONES	PG&E	0.8	-22.	RNCHSECO	PG&E	0.4
GEYSER B	PG&E	0.7	3.1	GEYSER C	PG&E	0.4
GEYSER D	PG&E	0.7	3.3	MOSS 7	PG&E	0.4
GEYSER A	PG&E	0.7	2.8	FCNGN4CC	ARIZ	0.3
GEYSER C	PG&E	0.7	3.3	GEYSER B	PG&E	0.3
FOLSOM1	PG&E	0.6	1.0	MELONES	PG&E	0.2
FOLSOM23	PG&E	0.6	0.4	GEYSER34	PG&E	0.2
POTRERO3	PG&E	0.6	1.6	PTS7SWNG	PG&E	0.2
HNTRS2-4	PG&E	0.6	1.0	DIABLO1	PG&E	0.2
PTSB 6	PG&E	0.6	-0.4	GEYSER78	PG&E	0.2
	"			DIABLO2	PG&E	0.2
	"					

RDGR2GEN	NEVAD	0.2	166.1			
NEWMANG6	N.MEX	0.2	146.6			
APACHCT3	ARIZ	0.3	149.2			
HOOVERN8	WAPA	0.3	149.7			
MOHAV2CC	S.CAL	0.3	153.2			
MOHAV1CC	S.CAL	0.3	153.2			
FCNGN4CC	ARIZ	0.3	164.2			
HOVEN5-7	WAPA	0.3	159.8			
FCNGN4CC	ARIZ	0.4	135.1			
MOHAV2CC	S.CAL	0.3	144.7			
MOHAV1CC	S.CAL	0.3	144.7			
HOVRA5-7	WAPA	0.3	161.7			
NEWMAN46	N.MEX	0.4	139.8			
BLNDL G1	UTAH	0.4	-170.			
HOVRA3A4	WAPA	0.5	157.7			

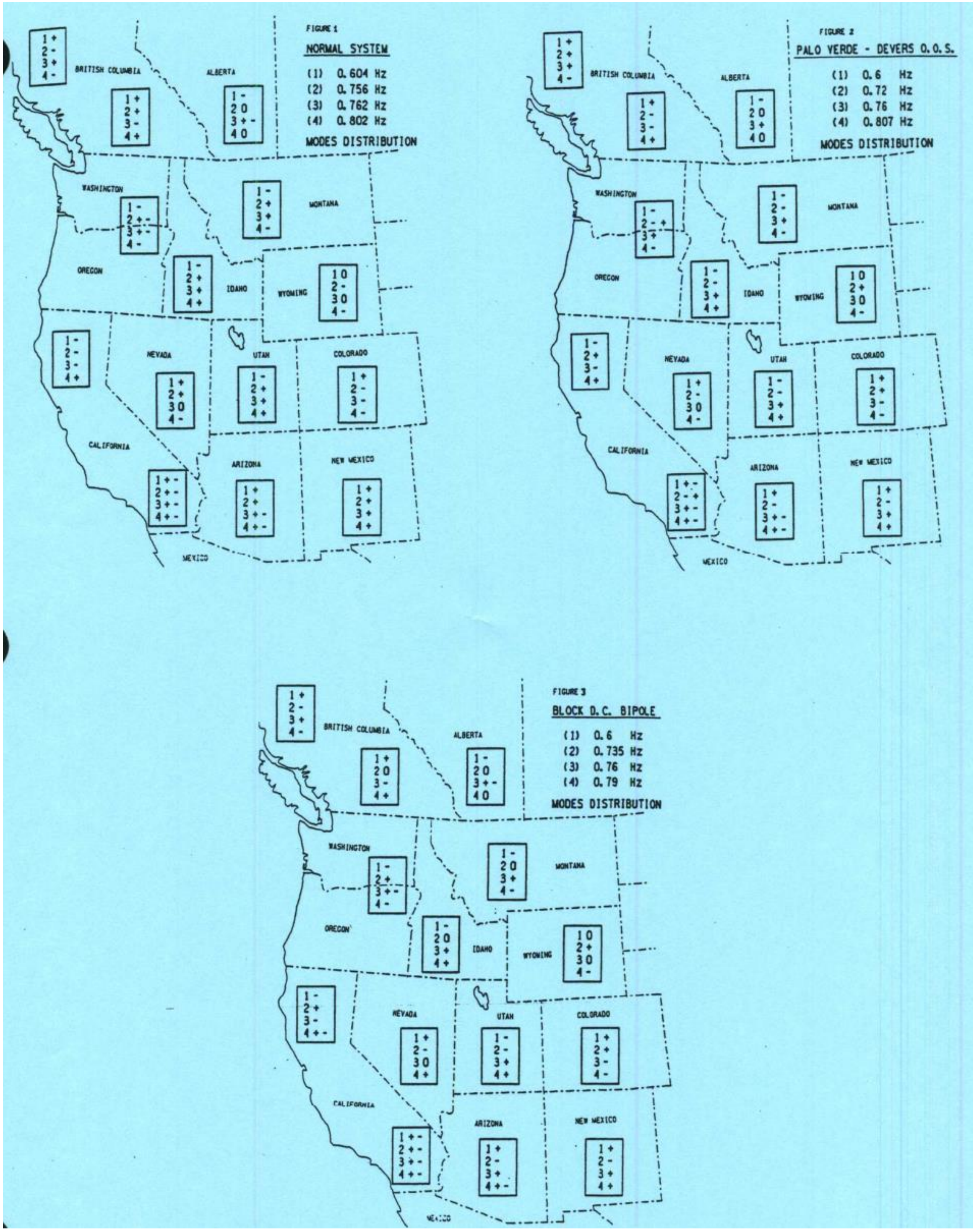

Finally, below is some work recently done reflecting mode shape in the Southwestern WECC system for a certain mode.

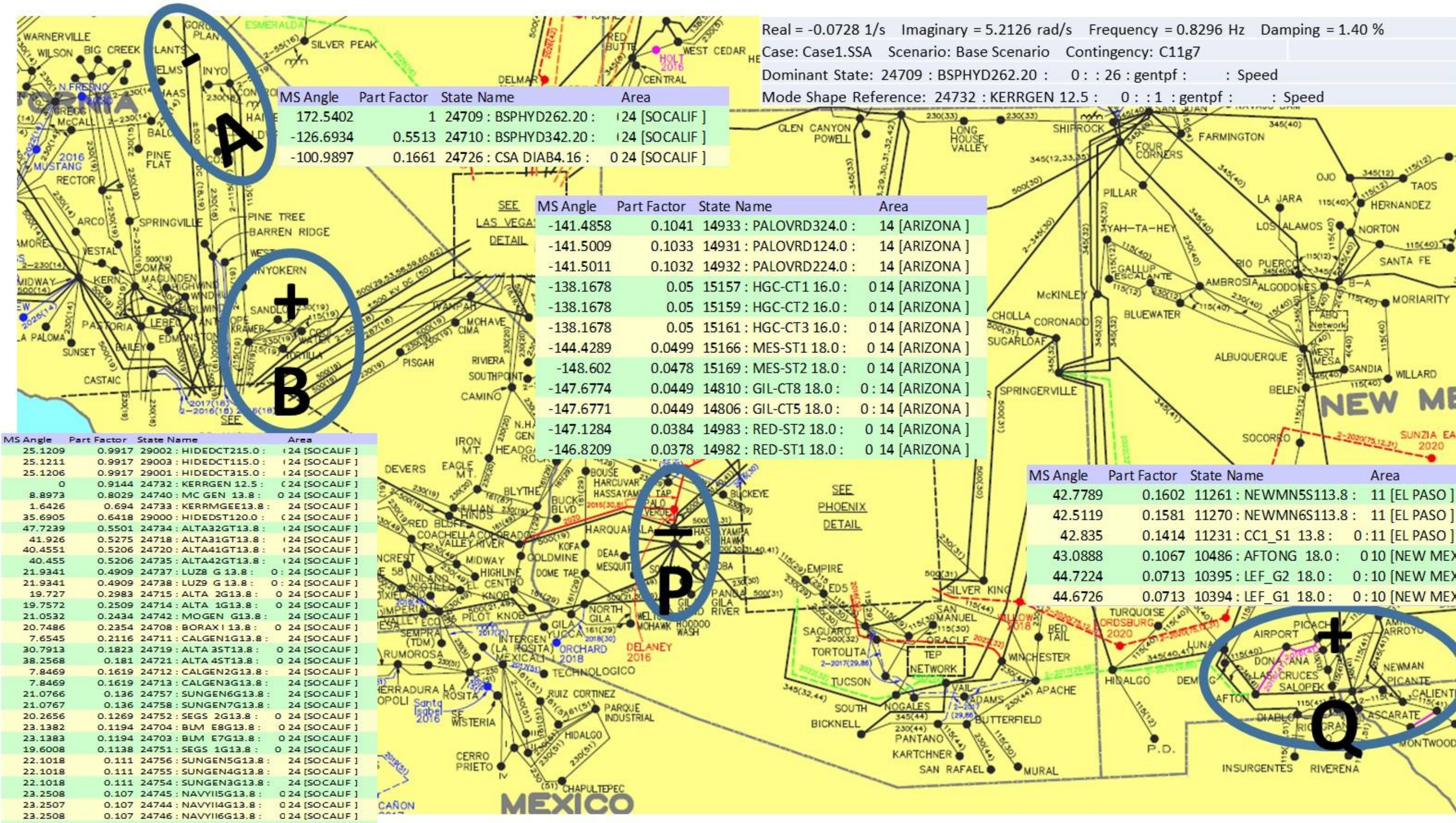

Real = -0.0728 1/s Imaginary = 5.2126 rad/s Frequency = 0.8296 Hz Damping = 1.40 %
Case: Case1.SSA Scenario: Base Scenario Contingency: C11g7
Dominant State: 24709 : BSPHYD262.20 : 0 : : 26 : gentpf : : Speed
Mode Shape Reference: 24732 : KERRGEN 12.5 : 0 : : 1 : gentpf : : Speed

MS Angle	Part Factor	State Name	Area
172.5402	1	24709 : BSPHYD262.20 :	(24 [SOCALIF]
-126.6934	0.5513	24710 : BSPHYD342.20 :	(24 [SOCALIF]
-100.9897	0.1661	24726 : CSA DIAB4.16 :	0 24 [SOCALIF]

MS Angle	Part Factor	State Name	Area
-141.4858	0.1041	14933 : PALOVRD324.0 :	14 [ARIZONA]
-141.5009	0.1033	14931 : PALOVRD124.0 :	14 [ARIZONA]
-141.5011	0.1032	14932 : PALOVRD224.0 :	14 [ARIZONA]
-138.1678	0.05	15157 : HGC-CT1 16.0 :	0 14 [ARIZONA]
-138.1678	0.05	15159 : HGC-CT2 16.0 :	0 14 [ARIZONA]
-138.1678	0.05	15161 : HGC-CT3 16.0 :	0 14 [ARIZONA]
-144.4289	0.0499	15166 : MES-ST1 18.0 :	0 14 [ARIZONA]
-148.602	0.0478	15169 : MES-ST2 18.0 :	0 14 [ARIZONA]
-147.6774	0.0449	14810 : GIL-CT8 18.0 :	0 : 14 [ARIZONA]
-147.6771	0.0449	14806 : GIL-CT5 18.0 :	0 : 14 [ARIZONA]
-147.1284	0.0384	14983 : RED-ST2 18.0 :	0 14 [ARIZONA]
-146.8209	0.0378	14982 : RED-ST1 18.0 :	0 14 [ARIZONA]

MS Angle	Part Factor	State Name	Area
25.1209	0.9917	29002 : HIDEDCT215.0 :	(24 [SOCALIF]
25.1211	0.9917	29003 : HIDEDCT115.0 :	(24 [SOCALIF]
25.1206	0.9917	29001 : HIDEDCT315.0 :	(24 [SOCALIF]
0	0.9144	24732 : KERRGEN 12.5 :	(24 [SOCALIF]
8.8973	0.8029	24740 : MC GEN 13.8 :	0 24 [SOCALIF]
1.6426	0.694	24733 : KERRMGEE13.8 :	24 [SOCALIF]
35.6905	0.6418	29000 : HIDEDST120.0 :	(24 [SOCALIF]
47.7239	0.5501	24734 : ALTA32GT13.8 :	(24 [SOCALIF]
41.926	0.5275	24718 : ALTA31GT13.8 :	(24 [SOCALIF]
40.4551	0.5206	24720 : ALTA41GT13.8 :	(24 [SOCALIF]
40.455	0.5206	24735 : ALTA42GT13.8 :	(24 [SOCALIF]
21.9341	0.4909	24737 : LUZ8 G 13.8 :	0 : 24 [SOCALIF]
21.9341	0.4909	24738 : LUZ9 G 13.8 :	0 : 24 [SOCALIF]
19.727	0.2983	24715 : ALTA 2G13.8 :	0 24 [SOCALIF]
19.7572	0.2509	24714 : ALTA 1G13.8 :	0 24 [SOCALIF]
21.0532	0.2434	24742 : MOGEN G13.8 :	24 [SOCALIF]
20.7486	0.2354	24708 : BORAX I 13.8 :	0 24 [SOCALIF]
7.6545	0.2116	24711 : CALGEN1G13.8 :	24 [SOCALIF]
30.7913	0.1823	24719 : ALTA 3ST13.8 :	0 24 [SOCALIF]
38.2568	0.181	24721 : ALTA 4ST13.8 :	0 24 [SOCALIF]
7.8469	0.1619	24712 : CALGEN2G13.8 :	24 [SOCALIF]
7.8469	0.1619	24713 : CALGEN3G13.8 :	24 [SOCALIF]
21.0766	0.136	24757 : SUNGEN6G13.8 :	24 [SOCALIF]
21.0767	0.136	24758 : SUNGEN7G13.8 :	24 [SOCALIF]
20.2656	0.1269	24752 : SEGS 2G13.8 :	0 24 [SOCALIF]
23.1382	0.1194	24704 : BLM E8G13.8 :	0 24 [SOCALIF]
23.1383	0.1194	24703 : BLM E7G13.8 :	0 24 [SOCALIF]
19.6008	0.1138	24751 : SEGS 1G13.8 :	0 24 [SOCALIF]
22.1018	0.111	24756 : SUNGEN5G13.8 :	24 [SOCALIF]
22.1018	0.111	24755 : SUNGEN4G13.8 :	24 [SOCALIF]
22.1018	0.111	24754 : SUNGEN3G13.8 :	24 [SOCALIF]
23.2508	0.107	24745 : NAVYII5G13.8 :	0 24 [SOCALIF]
23.2507	0.107	24744 : NAVYII4G13.8 :	0 24 [SOCALIF]
23.2508	0.107	24746 : NAVYII6G13.8 :	0 24 [SOCALIF]
23.5382	0.0871	24705 : BLM W9G13.8 :	(24 [SOCALIF]

MS Angle	Part Factor	State Name	Area
42.7789	0.1602	11261 : NEWMN5S113.8 :	11 [EL PASO]
42.5119	0.1581	11270 : NEWMN6S113.8 :	11 [EL PASO]
42.835	0.1414	11231 : CC1_S1 13.8 :	0 : 11 [EL PASO]
43.0888	0.1067	10486 : AFTONG 18.0 :	0 10 [NEW MEXI]
44.7224	0.0713	10395 : LEF_G2 18.0 :	0 : 10 [NEW MEXI]
44.6726	0.0713	10394 : LEF_G1 18.0 :	0 : 10 [NEW MEXI]